

Supporting Information

Near-infrared Emitting Single- and Mixed-Ligand MOFs that can Be Excited in the Visible Region: Synthesis, Crystal Structures and Sensitization of Nd³⁺, Er³⁺ and Yb³⁺

Athanasia E. Psalti,^a Despoina Andriotou,^a Svetlana V. Eliseeva,^{*b} Antonios Hatzidimitriou,^a Stephane Petoud^{*b} and Theodore Lazarides^{*a}

^a Department of Chemistry, Aristotle University of Thessaloniki, 54124 Thessaloniki, Greece.

^b Centre de Biophysique Moléculaire, CNRS UPR 4301, Université d'Orléans, rue Charles Sadron, 45071 Orléans, France

Table of Contents

Materials and methods	2
Physical methods	2
Synthesis of Ln-MOFs	3
Table S1. Selected bond lengths and angles of 2-LnANDC MOFs	4
Table S2. Selected crystal data for 1-NdNDC, 2-Ln ₁ ANDC ₁ (Ln = Nd, Yb, Er, Lu) and 2-ErDANDC	5
Figure S1. FTIR spectra of 2-LnANDC MOFs (Ln = Nd, Er, Yb and Lu)	6
Figure S2. FTIR spectra of 2-LnDANDC MOFs (Ln = Nd, Er and Yb)	6
Figure S3. TGA diagrams of (a) 1-Nd ₁ NDC and (b) 2-Nd ₁ ANDC ₁ MOFs	7
Figure S4. PXRD diagrams of 1-Ln _x ANDC _y MOFs. (a) Ln = Yb, x = 0 – 0.5; y = 0 – 0.2 and (b) Ln = Nd, x = 0 – 0.2.	8
Figure S5. Simulated and measured PXRD diagrams of (a) 2-LnDANDC and (b) 2-LnANDC, Ln = Yb, Er, Nd.	9
Figure S6. (a) Excitation spectra ($\lambda_{em} = 1064$ nm), (b) diffuse reflectance spectra and (c) emission spectra ($\lambda_{exc} = 350$ nm) of 1-NdANDC _x MOFs (x = 0–0.2).	10
Figure S7. (a) Excitation spectra ($\lambda_{em} = 980$ nm), (b) diffuse reflectance spectra and (c) emission spectra ($\lambda_{exc} = 350$ nm) of 1-Yb _x ANDC _y MOFs (x = 0.2, y = 0.005–0.5).	11
Figure S8. Excitation, emission and absorption spectra of the ligands. (a) H ₂ ANDC and (b) H ₂ DANDC in methanol solutions (10 ⁻⁵ M).	12
Figure S9 Diffuse reflectance spectra of 2-Nd ₁ ANDC ₁ (red trace), 2-NdDANDC (blue trace) and emission spectra of methanol solutions (10 ⁻⁵ M) of H ₂ ANDC (green line) and H ₂ DANDC (black line)	13
Figure S10 Diffuse reflectance spectra of 2-Nd ₁ ANDC ₁ , 2-NdDANDC and 1-Nd ₁ NDC, 20% w/w in BaSO ₄	13
Figure S11. Experimental steady-state (a, c, e) and time-gated (b, d, f) (time delay 1 μ s) emission spectra of (a, b) 1-LaNDC, (c, d) 1-LaANDC _{0.03} and (e, f) 1-LaDANDC _{0.02} in the solid state (77K, white circles), and corresponding Gaussian deconvolution (red and green traces) to determine the energies of the corresponding ligand excited states.	14
Exciton migration studies	15

Synthesis of mixed-ligand LnMOFs	15
Table S3. Quantum yield measurements of $[La_1(NDC)_{1-y}(ANDC)_yCl(DMF)]$ and $[La_1(NDC)_{1-y}(DANDC)_yCl(DMF)]$ ($y = 0 - 0.01$).	15
References	15

Materials and methods

All commercially available starting reagents and solvents were purchased from the usual sources and were used as received.

1-aminonaphthalene-3,7-dicarboxylic acid (H_2ANDC) was prepared according to published procedures.¹ The 1H -NMR spectrum of the product agreed with the one reported in the literature: 1H -NMR: (DMSO- d_6 , 500 MHz): δ (ppm) 12,89 (br, 2H), 8,79 (1H, s), 7,94 (1H, d), 7,89 (1H, d), 7,74 (1H, s), 7,23 (1H, s), 6,23 (2H, s).

4,8-diaminonaphthalene-2,6-dicarboxylic (H_2DANDC) acid was prepared according to the published procedures.² The 1H -NMR spectrum of the product agreed with the one reported in the literature: 1H NMR (500 MHz, DMSO- d_6): δ (ppm) = 7.90 (s, 2 H), 7.16 (s, 2 H), 5.82 (br, 4 H).

Physical methods

PXRD data were collected at ambient temperature using a Bruker D8 Advance X-ray diffractometer with a Cu $K\alpha$ source ($\lambda = 1.5418 \text{ \AA}$).

The **single crystal X-ray** diffraction studies were carried out on carefully chosen single crystals which were coated with Paratone-N oil before being mounted on the goniometer of a Bruker Kappa Apex-II CCD diffractometer, using graphite-monochromatized Mo $K\alpha$ radiation ($\lambda = 0.7107 \text{ \AA}$).³ Data collection details can be found in Table S2 and the respective crystallographic information files. The structures were solved by direct methods with SUPERFLIP and refined on F^2 by full matrix least squares method in the anisotropic approximation (for non-hydrogen atoms) using the CRYSTALS program suite.⁴⁻⁹ Images were produced using the Mercury software from CCDC.¹⁰

UV-visible-NIR diffuse reflectance spectra in the solid state were obtained using a JASCO V-750 spectrophotometer equipped with an INS-470 integrating sphere attachment at ambient temperature.

Nanosecond time-resolved experiments were performed using an Edinburgh Instruments mini- τ lifetime spectrometer with bandpass filters (± 40 nm bandpass) at 450, 500, 600 and 650 nm. The excitation source was an Edinburgh Instruments picosecond pulsed LED (EPLD-320) with a maximum wavelength at 326.8 nm and a pulse width of 910 ps. The detector was a thermoelectrically cooled, high-speed red-sensitive photomultiplier tube (Hamamatsu H10720-01). The Instrument Response Function (IRF) was collected using a sample consisting of water with a few drops of colloidal silica (LUDOXTM-Aldrich) scattering medium in an open filter configuration. The data were analyzed using the software provided by the manufacturer (FLUORACLE).

NIR luminescence studies were performed at room temperature on samples in the solid state placed into quartz capillaries with 2 mm i.d. Steady-state emission and excitation spectra were measured on a custom-designed Horiba Scientific Fluorolog 3-22 spectrofluorimeter equipped with a visible

photomultiplier tube (PMT) (220–950 nm, R13456; Hamamatsu) and a NIR PMT (950–1650 nm, H10330-75; Hamamatsu) upon excitation with a continuous Xenon lamp. All excitation and emission spectra were corrected for the instrumental functions.

Absolute quantum yields in the NIR range were determined with the Fluorolog 3 spectrofluorimeter based on an absolute method with the use of an integration sphere (Model G8, GMP SA, Renens, Switzerland). Estimated experimental error for quantum yield determination is ~10 %.

Luminescence lifetimes (τ_{obs}) were determined under excitation at 355 nm provided by a Nd:YAG laser (YG 980; Quantel). The signal was selected using an iHR320 monochromator (Horiba Scientific) and detected with a Hamamatsu H10330-75 PMT.

Luminescence studies in the visible range were conducted in the steady-state mode using an FS5 Edinburgh instruments spectrofluorometer with a Hamamatsu R13456 photomultiplier tube detector and a 150W Xenon arc lamp as an excitation source. Quantum yields were measured using the SC-30 integration sphere accessory. The spectra were plotted and analyzed using the FLUORACLE software. Spectral corrections supplied by the manufacturer were applied to all measured spectra.

Synthesis of Ln-MOFs

Synthesis of 1-LaNDC MOF: $\text{LnCl}_3 \cdot x\text{H}_2\text{O}$ (0.05 mmol) and 2,6-naphthalenedicarboxylic acid (0.05 mmol) were added as solids in DMF (3 mL). The resulting solution was sealed in a screw cap 23 mL scintillation vial and placed in a preheated oven at 110°C where it remained undisturbed for 24 h before being cooled to room temperature. Colorless rod-like crystals were washed with DMF (5 × 3 mL) and stored in DMF (yield, 45%). **Mixed-metal mixed-ligand 1-Ln_xANDC_y MOFs (Ln = Nd³⁺, Yb³⁺, y = 0 – 0.2, x = 0.005 – 1)** were synthesized by adding specific quantities of 0.03 M stock solutions of $\text{LnCl}_3 \cdot x\text{H}_2\text{O}$ and H_2ANDC in DMF to the reaction mixture using an automatic pipette.

Synthesis of 2-LnANDC and 2-LnDANDC MOFs: $\text{Ln}(\text{NO}_3)_3 \cdot x\text{H}_2\text{O}$ (0.05mmol) and 1-aminonaphthalene-3,7-dicarboxylic acid (17.83 mg, 0.075 mmol) or 4,8-diaminonaphthalene-2,6-dicarboxylic acid (0.075 mmol) were added as solids into 3 mL of solvents mixture, DMF/H₂O/EtOH (10:1:1). The resulting solution was sealed in a scintillation vial and placed in a preheated oven at 70°C, remaining undisturbed at this temperature for 72 h before being cooled gradually to room temperature. The block-shaped yellow crystals were washed with DMF (5 × 3 mL) and stored in DMF (yield, 38%).

Table S1. Selected bond lengths and angles of 2-LnANDC MOFs.

2-NdANDC	Distance (Å)	2-ErANDC	Distance (Å)	2-YbANDC	Distance (Å)	2-LuANDC	Distance (Å)
Nd1-O1	2.41	Er1-O1	2.338	Yb1-O1	2.299	Lu1-O1	2.293
Nd1-O1	2.709	Er1-O2	2.791	Yb1-O2	2.285	Lu1-O2	2.209
Nd1-O2	2.477	Er1-O2	2.256	Yb1-O3	2.373	Lu1-O3	2.369
Nd1-O3	2.443	Er1-O3	2.401	Yb1-O4	2.412	Lu1-O4	2.393
Nd1-O4	2.428	Er1-O4	2.412	Yb1-O5	2.294	Lu1-O5	2.290
Nd1-O5	2.528	Er1-O5	2.323	Yb1-O6	2.216	Lu1-O6	2.283
Nd1-O6	2.507	Er1-O6	2.323				
Nd1-Nd1	4.052	Er1-Er1	4.011	Yb1-Yb1	4.072	Lu1-Lu1	4.040
	Angle (°)		Angle (°)		Angle (°)		Angle (°)
Nd-O1-Nd	104.52	Er-O2-Er2	104.7	-	-	-	-
O3-C7-O4	126.37	O6-C13-O5	126.01	O1-C1-O2	127.36	C6-O13-C5	125.35
O1-Nd1-O2	49.18	O1-Er1-O2	49.30	-	-	-	-
O5-Nd1-O6	52.01	O3-Er1-O3	53.60	O3-Yb1-O4	54.34	O4-Lu1-O3	54.68
Nd1-C7-Nd1	71.97	Er1-C13-Er1	73.54	Yb1-C1-Yb1	75.48	Lu1-C13-Lu1	74.82

Table S2. Selected crystal data for 1-NdNDC, 2-Ln₁ANDC₁ (Ln = Nd, Yb, Er, Lu) and 2-ErDANDC.

Compound	1-Nd ₁ NDC	2-Nd ₁ ANDC ₁	2-Yb ₁ ANDC ₁	2-Er ₁ ANDC ₁	2-Lu ₁ ANDC ₁	2-ErDANDC
CCDC No	2312506	2312507	2312509	2312508	2312510	2312511
Chemical formula	C ₁₅ H ₁₃ ClNNdO ₅	C _{54.00} H _{60.00} N _{9.00} Nd ₂ O _{18.00}	C ₅₇ H ₆₇ N ₁₀ O ₁₉ Y b ₂	C ₂₇ H _{31.50} ErN _{4.50} O _{9.75}	C ₂₇ H ₃₁ LuN _{4.50} O 9.50	C _{28.50} H _{36.50} ErN ₆ .50O _{9.50}
Formula mass	466.96	1411.58	1542.29	742.33	745.54	789.40
Crystal system	Orthorhombic	Triclinic	Triclinic	Triclinic	Triclinic	Triclinic
a (Å)	7.6570 (3)	12.2616 (7)	12.018 (3)	11.7875 (14)	11.7299 (13)	12.205 (2)
b (Å)	21.2979 (8)	12.2946 (6)	12.3018 (14)	12.2352 (15)	12.2689 (15)	12.2078 (18),
c (Å)	9.7601 (4)	13.5256 (8)	13.2497 (18)	13.3056 (14)	13.2149 (14)	13.309 (2)
α (°)	90	102.201 (3)	104.019 (9)	103.963 (3)	104.281 (3)	105.069 (5)
β (°)	90	99.667 (3)	99.232 (14)	99.129 (3)	98.937 (3)	100.428 (5)
γ (°)	90	103.240 (3)	100.251 (13)	100.537 (4)	99.454 (4)	98.173 (5)
Unit cell volume (Å ³)	1591.66 (11)	1889.16 (19)	1827.2 (6)	1789.0 (4)	1779.4 (4)	1845.3 (5)
Temperature (K)	295	130	130	135	135	135
Space group	Pnma	<i>P</i> -1	<i>P</i> -1	<i>P</i> -1	<i>P</i> -1	<i>P</i> -1
Z	4	1	1	2	2	2
No. of reflections measured	18962	24937	22108	27882	28158	27848
No. of independent reflections	2636	7240	6712	6861	6851	7081
No. of observed reflections [I>2.0σ(I)]	1964	5321	5030	5170	4827	4759
R _{int}	0.037	0.019	0.046	0.032	0.056	0.078
R [F ² >2σ(F ²)]	0.035	0.029	0.033	0.034	0.035	0.039
wR(F ²)	0.070	0.065	0.080	0.082	0.082	0.087

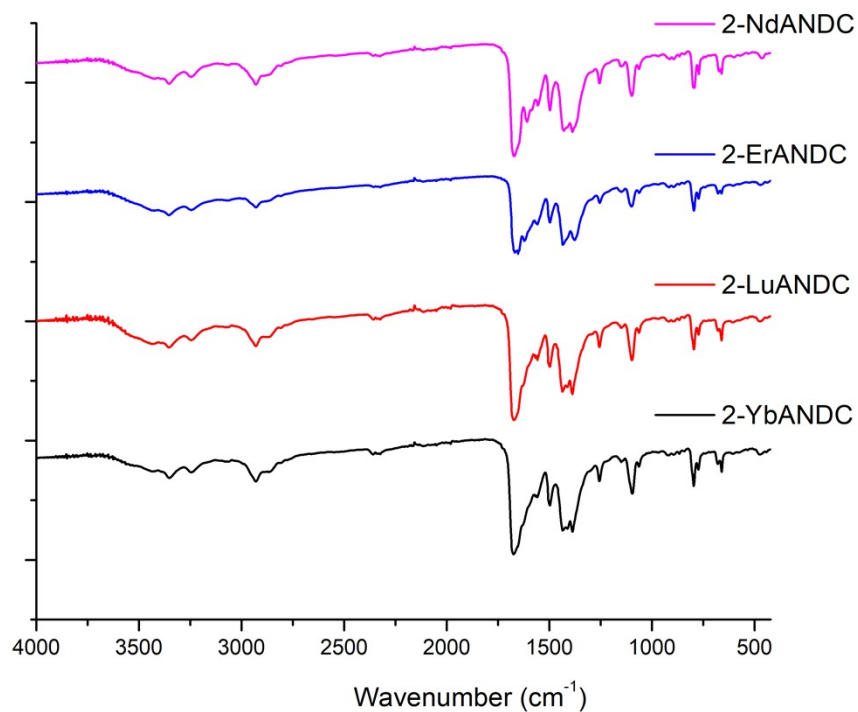


Figure S1. FTIR spectra of 2-LnANDC MOFs (Ln = Nd, Er, Yb and Lu).

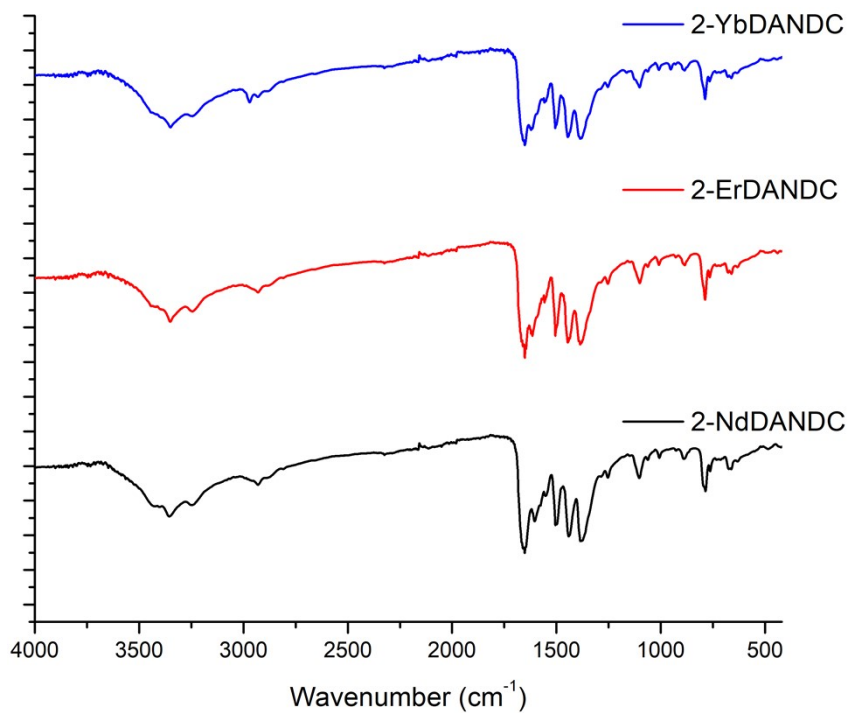


Figure S2. FTIR spectra of 2-LnDANDC MOFs (Ln = Nd, Er and Yb).

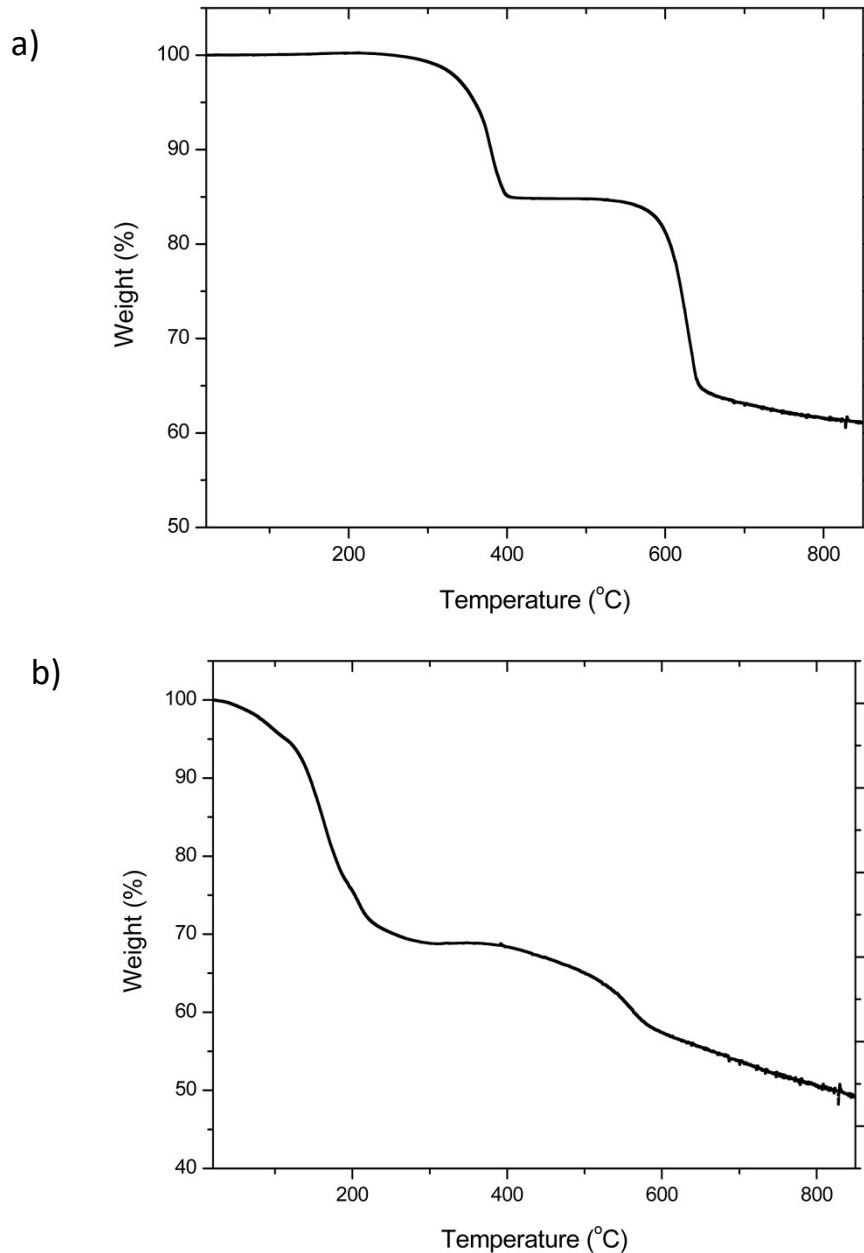
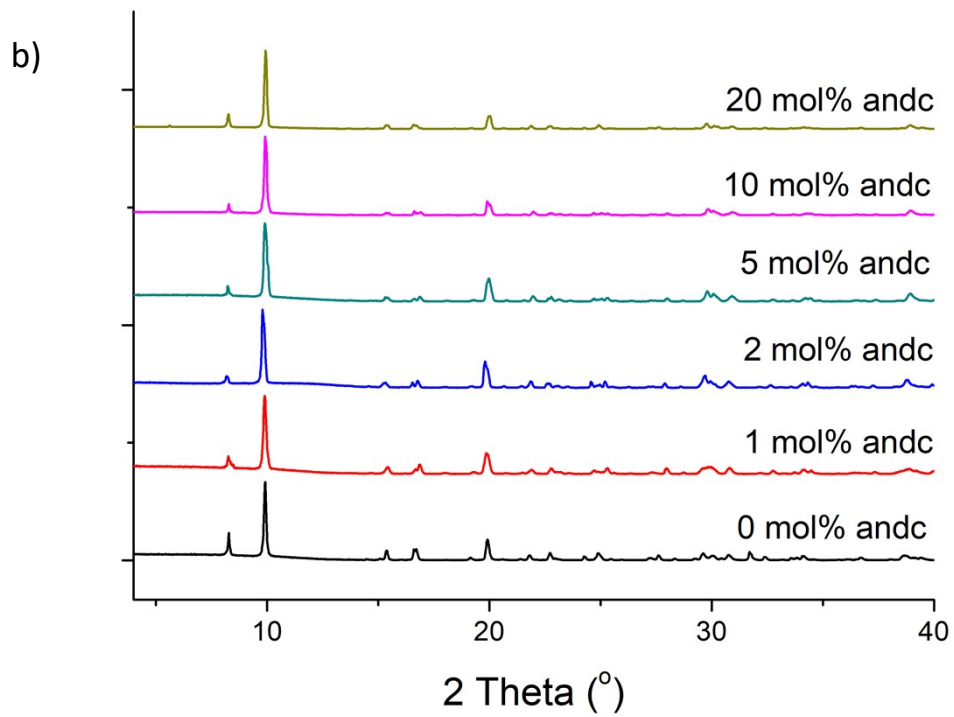
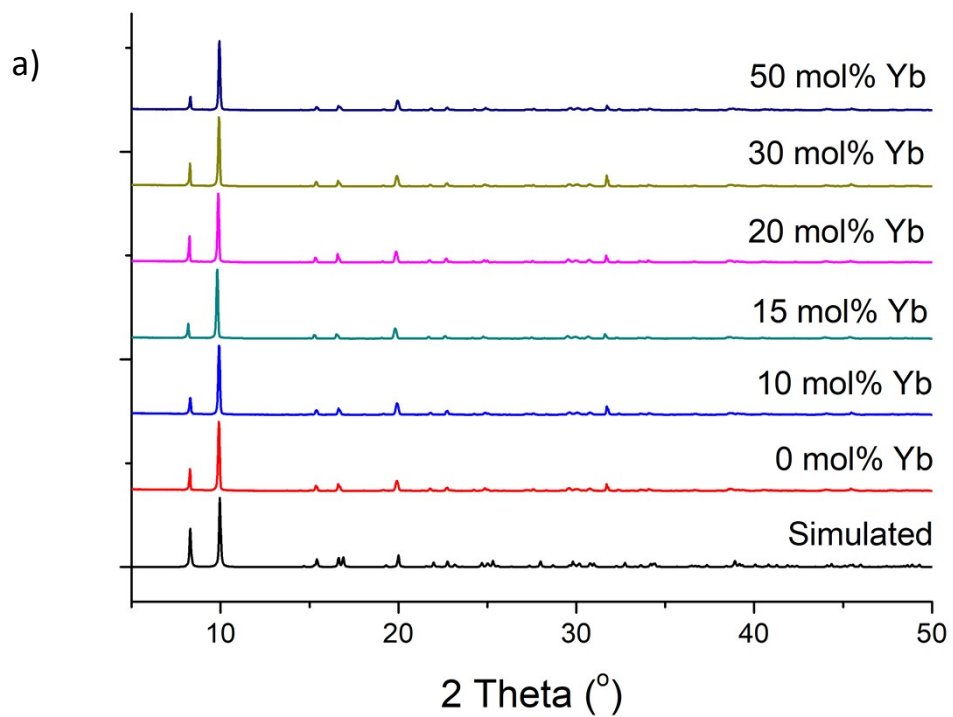


Figure S3. TGA diagrams of (a) 1-Nd₁NDC and (b) 2-Nd₁ANDC₁ MOFs.

TGA data of 1-Ln_xANDC_y (Figure S3a) indicate the weight losses starting from 272 °C and ending at over 700 °C in two stages. In the first step (25–396 °C) we observe the weight loss of one terminally coordinated DMF molecule (experimental loss of 15.4%, theoretically estimated 15.8%) followed by a thermally stable intermediate. The framework decomposes at 650 °C. 2-Ln_xANDC_y MOFs (Figure S3b) show weight loss starting from 170 °C and ending at over 800 °C in two steps. In the first step (170– 220 °C) we observe the weight losses of one guest DMF molecule and a terminally coordinated DMF molecule (experimental weight loss of 27%, theoretically estimated loss of 30.7%). Finally, the framework decomposes at 570 °C.



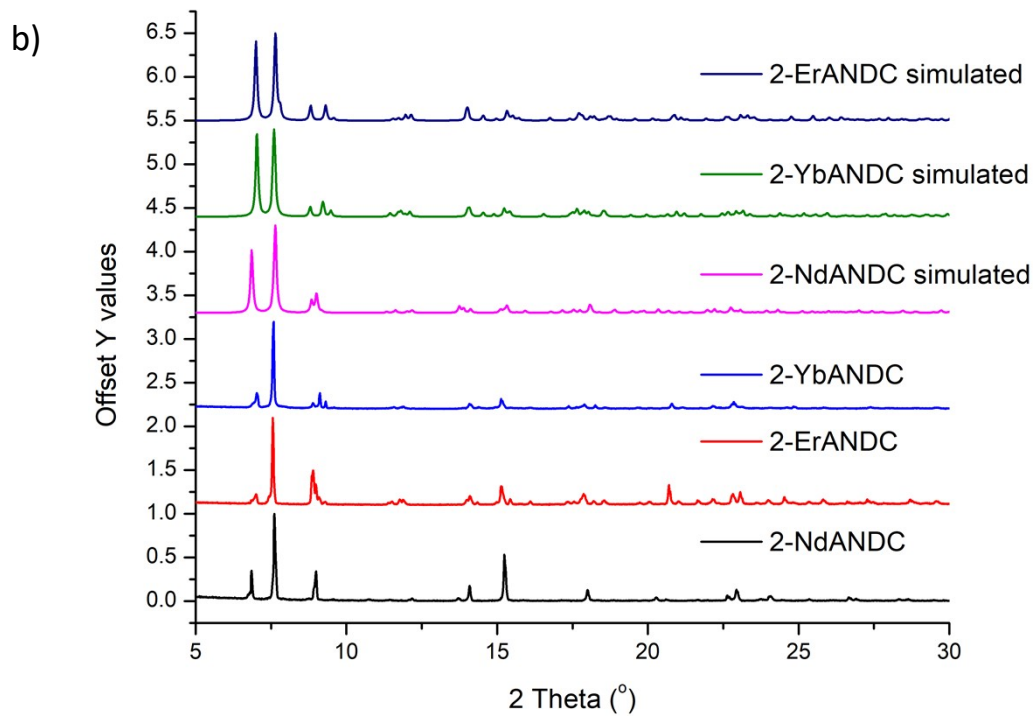
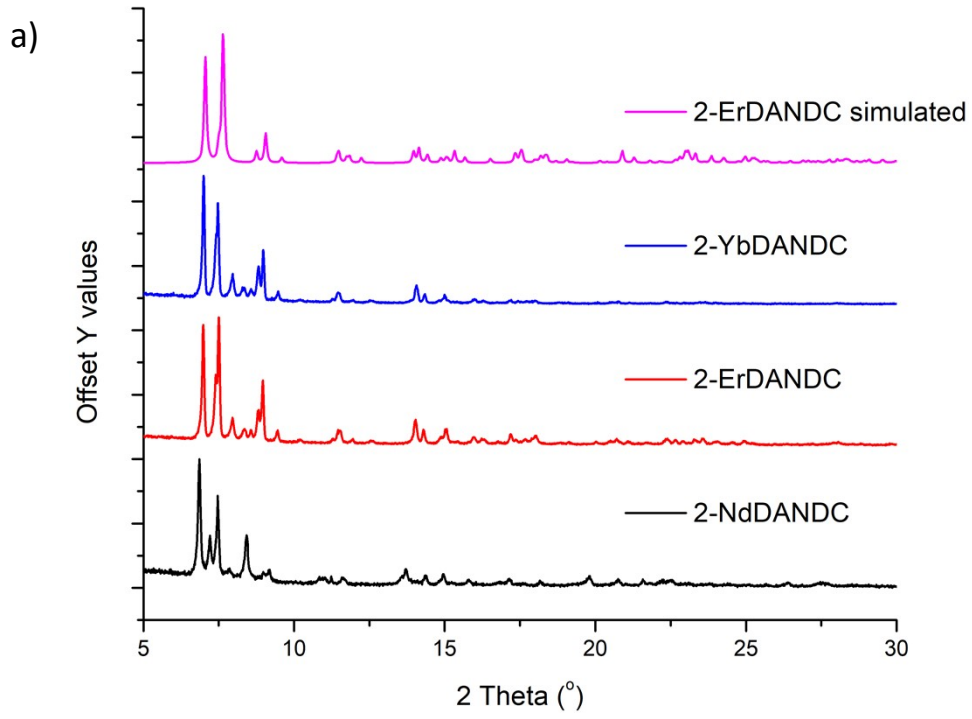


Figure S5. Simulated and measured PXRD diagrams of (a) 2-LnDANDC and (b) 2-LnANDC, Ln = Yb, Er, Nd.

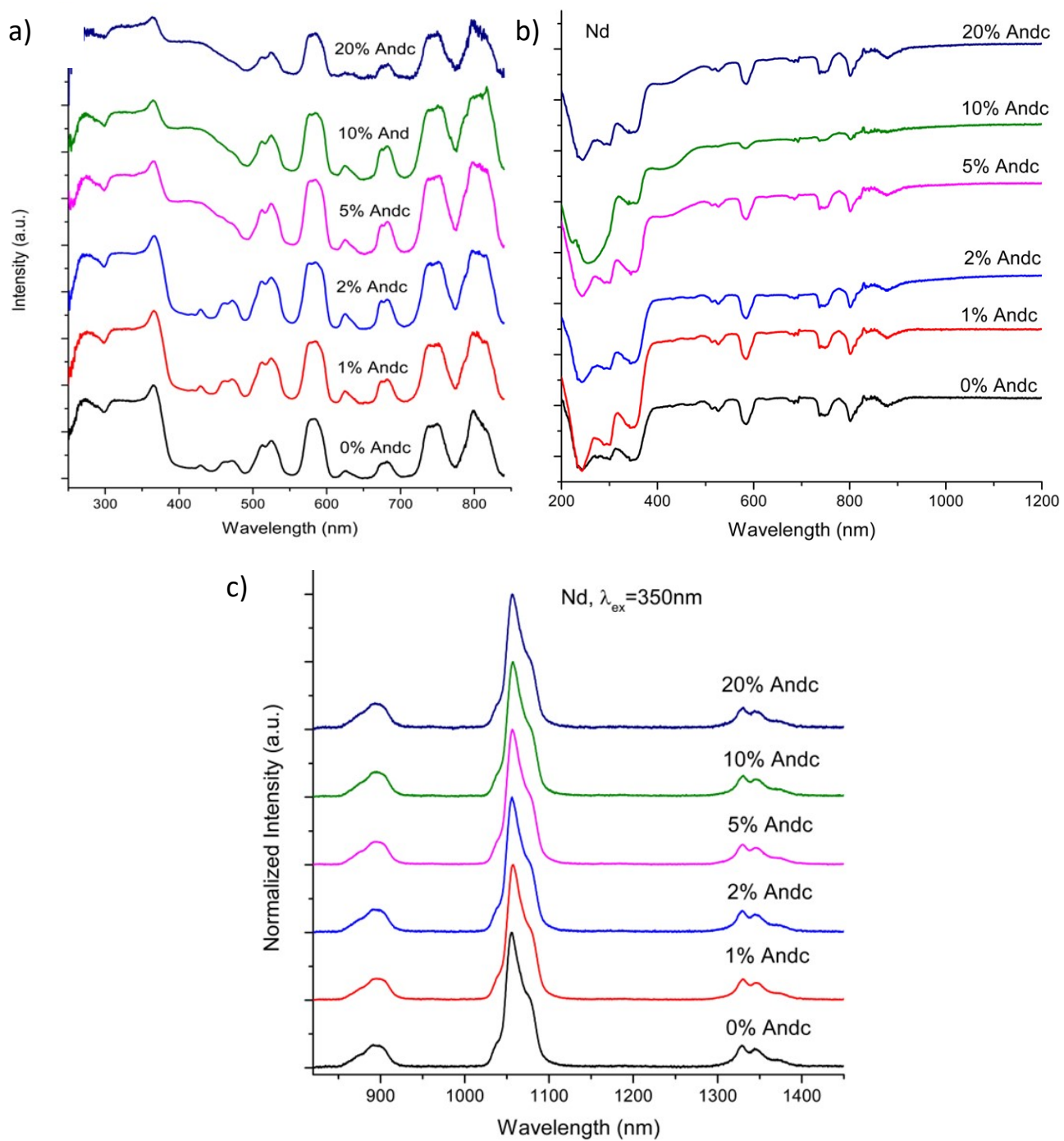


Figure S6. (a) Excitation spectra ($\lambda_{\text{em}} = 1064 \text{ nm}$), (b) diffuse reflectance spectra and (c) emission spectra ($\lambda_{\text{exc}} = 350 \text{ nm}$) of 1-NdANDC_x MOFs ($x = 0\text{--}0.2$).

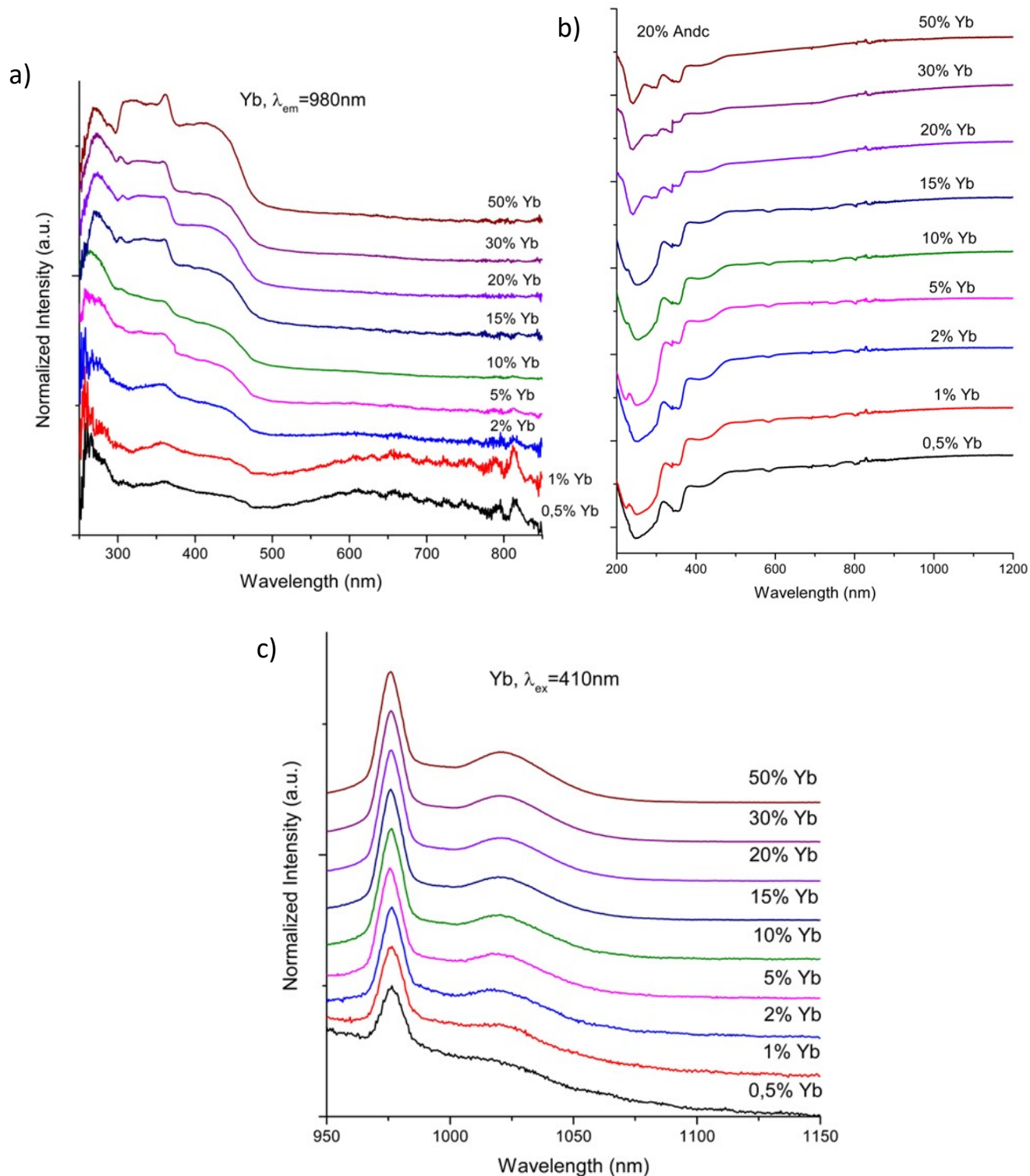


Figure S7. (a) Excitation spectra ($\lambda_{em} = 980\text{ nm}$), (b) diffuse reflectance spectra and (c) emission spectra ($\lambda_{exc} = 350\text{ nm}$) of $1\text{-Yb}_x\text{ANDC}_y$ MOFs ($x = 0.2$, $y = 0.005\text{-}0.5$).

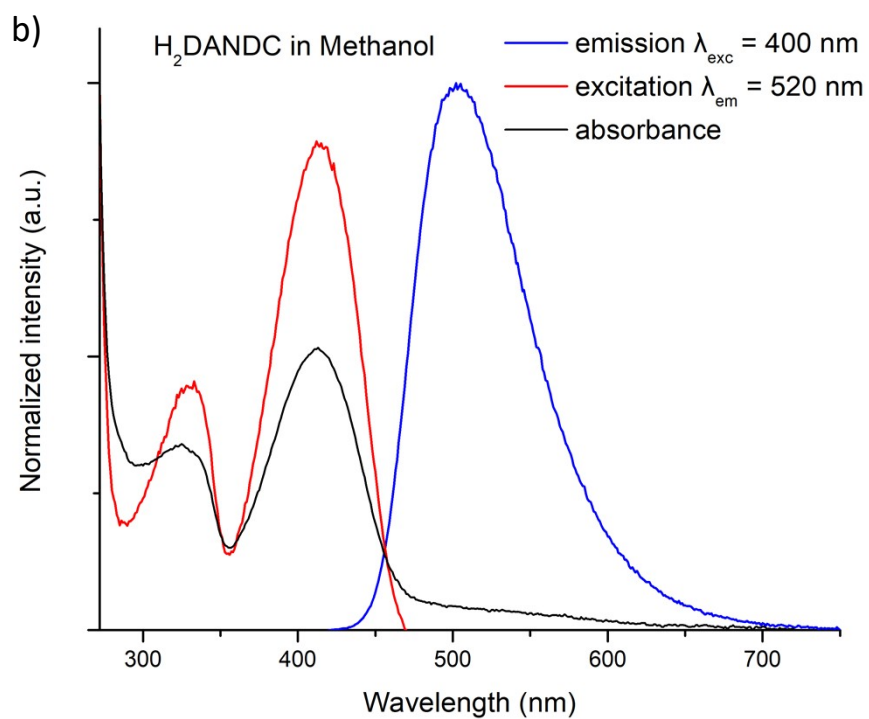
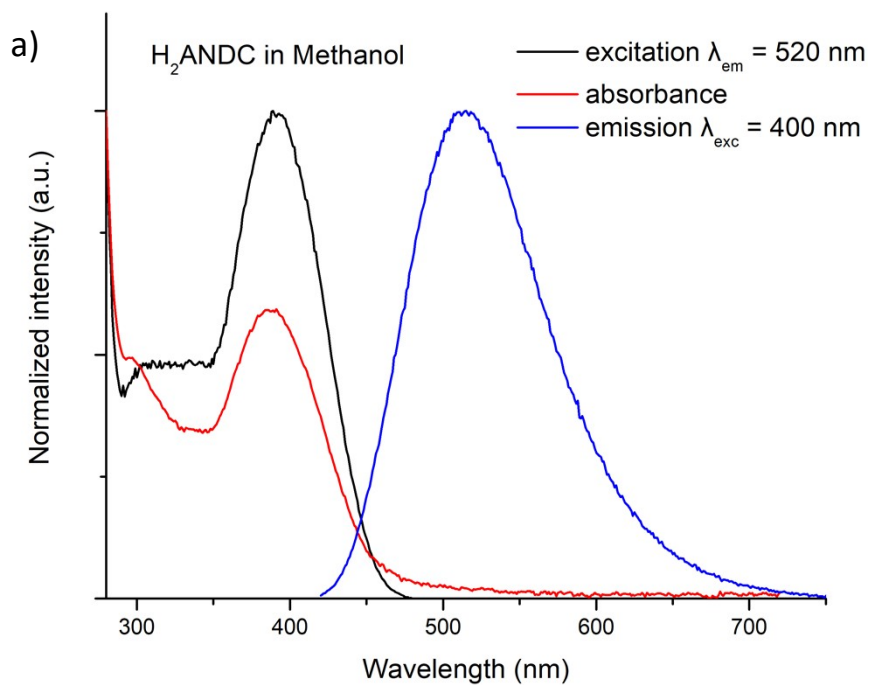


Figure S8. Excitation, emission and absorption spectra of the ligands. (a) H_2ANDC and (b) H_2DANDC in methanol solutions (10^{-5} M).

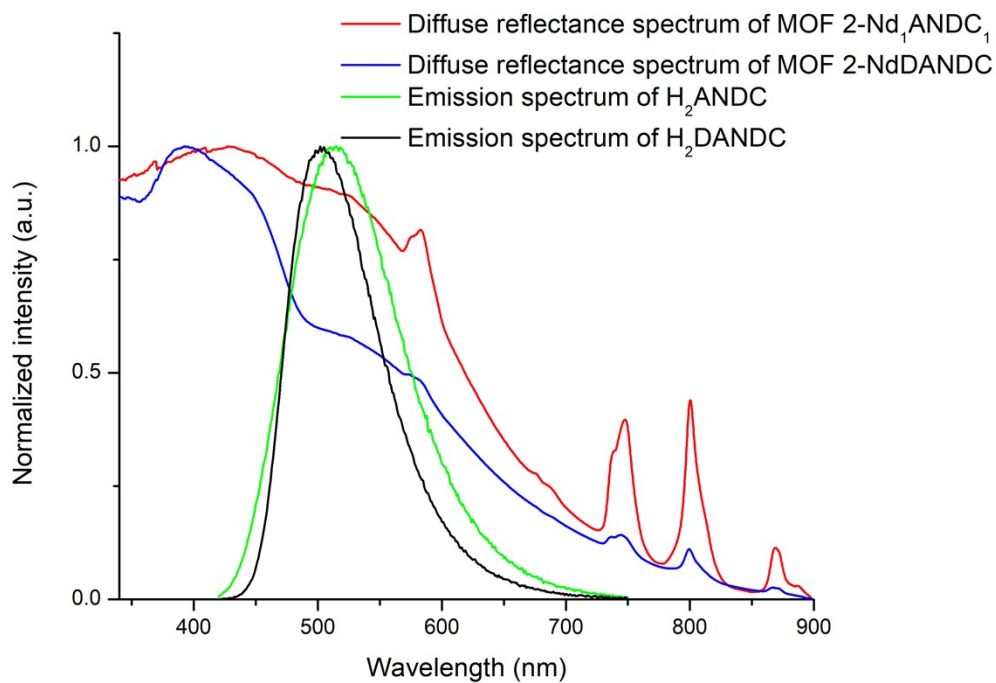


Figure S9 Diffuse reflectance spectra of 2-Nd₁ANDC₁ (red trace), 2-NdDANDC (blue trace) and emission spectra of methanol solutions (10⁻⁵ M) of H₂ANDC (green line) and H₂DANDC (black line).

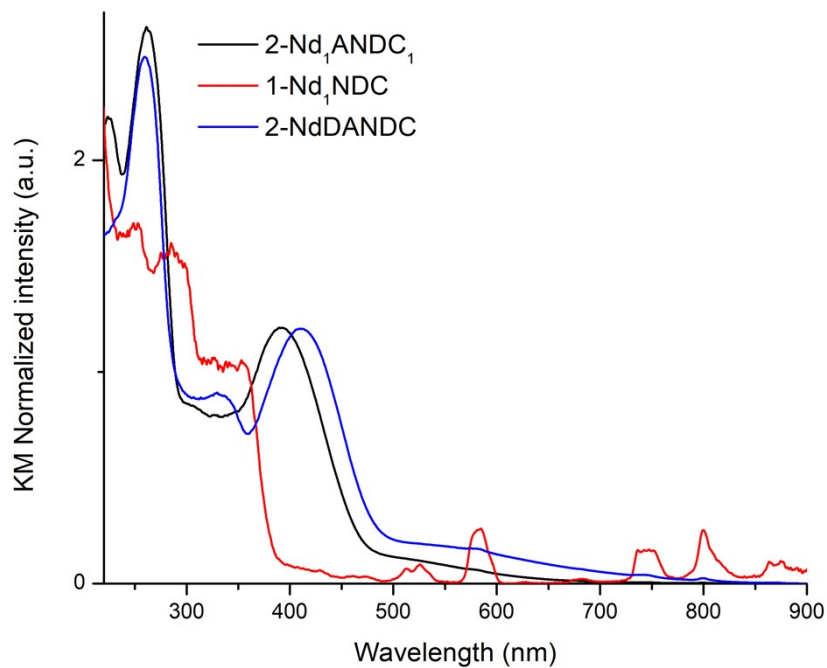


Figure S10 Diffuse reflectance spectra of 2-Nd₁ANDC₁, 2-NdDANDC and 1-Nd₁NDC, 20% w/w in BaSO₄.

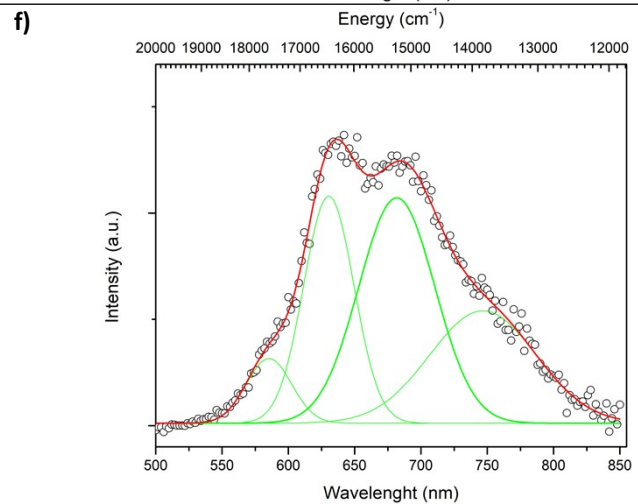
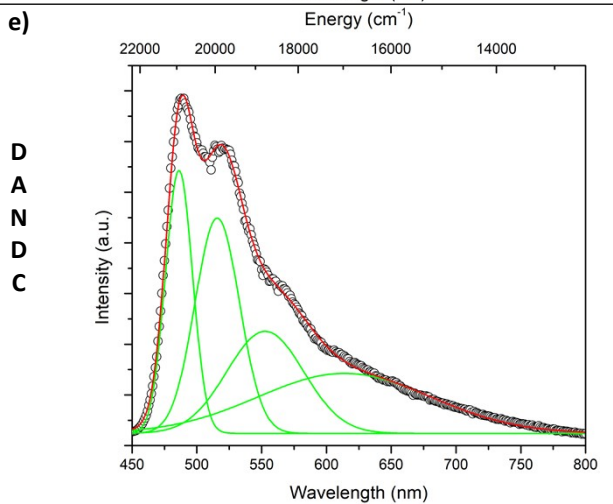
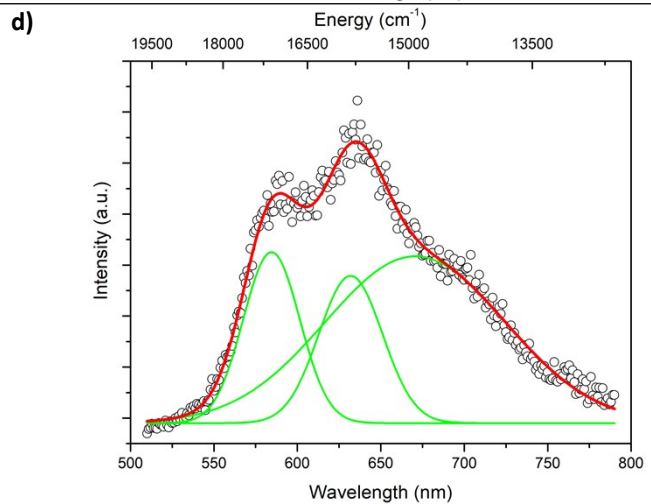
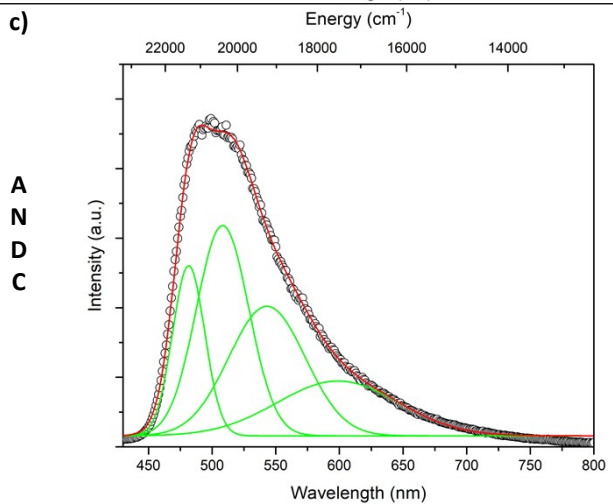
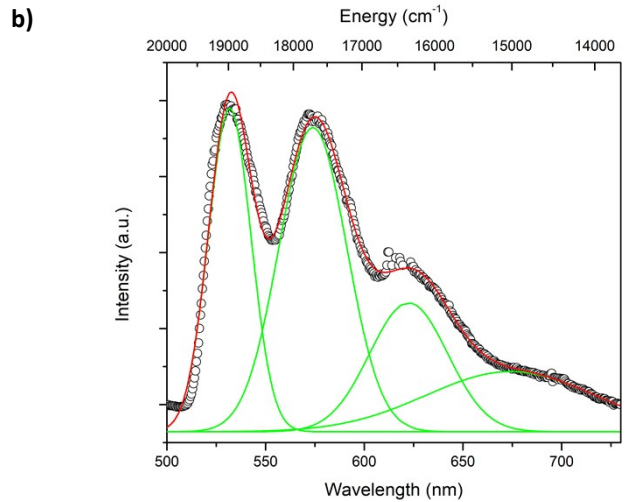
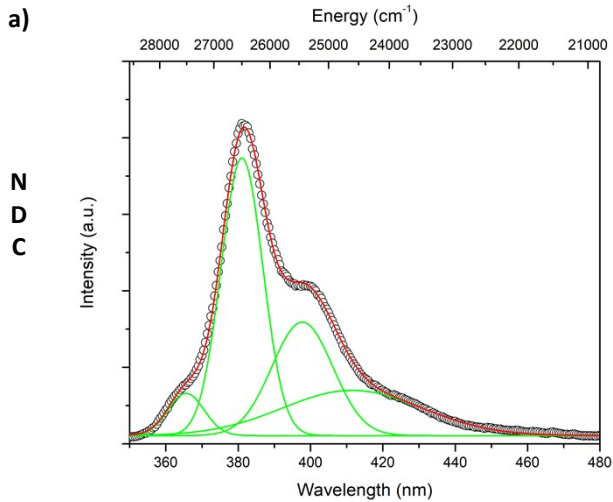


Figure S11. Experimental steady-state (a, c, e) and time-gated (b, d, f) (time delay 1 μ s) emission spectra of (a, b) 1-LaNDC, (c, d) 1-LaANDC_{0.03} and (e, f) 1-LaDANDC_{0.02} in the solid state (77K, white circles), and corresponding Gaussian deconvolution (red and green traces) to determine the energies of the corresponding ligand excited states.

Exciton migration studies

Synthesis of mixed-ligand LnMOFs

Synthesis of 1-LaNDC MOF: LnCl₃·xH₂O (0.05 mmol) and 2,6-naphthalenedicarboxylic acid (0.05 mmol) were added as solids in DMF (3 mL). The resulting solution was sealed in a screw cap 23 mL scintillation vial and placed in a preheated oven at 110°C where it remained undisturbed for 24 h before being cooled to room temperature. Colorless rod-like crystals were washed with DMF (5 × 3 mL) and stored in DMF (yield, 45%). **Mixed-ligand** [La₁(NDC)_{1- γ} (ANDC) _{γ} Cl(DMF)] and [La₁(NDC)_{1- γ} (DANDC) _{γ} Cl(DMF)] ($\gamma = 0 - 0.01$) were synthesized by adding specific quantities of 0.01 M stock solutions of H₂ANDC and H₂DANDC in DMF to the reaction mixture using an automatic micropipette.

Table S3. Quantum yield measurements of [La₁(NDC)_{1- γ} (ANDC) _{γ} Cl(DMF)] and [La₁(NDC)_{1- γ} (DANDC) _{γ} Cl(DMF)] ($\gamma = 0 - 0.01$).

ANDC				DANDC			
mol% ANDC	Molar fraction of ANDC	Φ^L (%)	Φ_0^L/Φ^L	mol% DANDC	Molar fraction of DANDC	Φ^L (%)	Φ_0^L/Φ^L
0	0	22.65(2)	1	0	0	22.65(2)	1
0.02	0.0002	16.58(7)	1.366	0.02	0.0002	15.99(3)	1.416
0.05	0.0005	13.01(3)	1.740	0.05	0.0005	10.47(2)	2.135
0.1	0.001	9.38(1)	2.414	0.1	0.001	6.8(3)	3.330
0.2	0.002	6.44(4)	3.517	0.2	0.002	4.35(7)	5.206
0.3	0.003	1.48(7)	15.304	0.3	0.003	3.04(7)	7.450
0.4	0.004	1.09(2)	20.77	0.4	0.004	1.82(2)	12.445
0.6	0.006	0.56(3)	40.44	0.6	0.006	1.27(1)	17.834
0.8	0.008	0.38(2)	59.605	0.8	0.008	1.17(4)	19.358
1	0.01	0.36(1)	62.916	1	0.01	0.75(5)	30.2

References

- 1 J. Sim, H. Yim, N. Ko, S. B. Choi, Y. Oh, H. J. Park, S. Park and J. Kim, *Dalton Transactions*, 2014, **43**, 18017–18024.
- 2 S. A. Diamantis, A. Hatzidimitriou, A. K. Plessas, A. Pournara, M. J. Manos, G. S. Papaefstathiou and T. Lazarides, *Dalton Trans.*, 2020, **49**, 16736–16744.

- 3 Bruker Analytical X-ray Systems, Inc., 2006. Apex2, Version 2 User Manual, M86-E01078, Madison, WI.
- 4 P. W. Betteridge, J. R. Carruthers, R. I. Cooper, K. Prout and D. J. Watkin, *J Appl Crystallogr*, 2003, **36**, 1487.
- 5 J. de Meulenaer and H. Tompa, *Acta Crystallogr*, 1965, **19**, 1014–1018.
- 6 L. Palatinus and G. Chapuis, *J Appl Crystallogr*, 2007, **40**, 786–790.
- 7 E. J. W. Whittaker, *Mineral Mag*, 1983, **47**, 262–263.
- 8 D. Watkin, *Acta Crystallographica Section A*, 1994, **50**, 411–437.
- 9 D. J. Watkin, C. K. Prout and L. J. Pearce, *Chemical Crystallography Laboratory, Oxford, UK*.
- 10 C. F. Macrae, I. Sovago, S. J. Cottrell, P. T. A. Galek, P. McCabe, E. Pidcock, M. Platings, G. P. Shields, J. S. Stevens, M. Towler and P. A. Wood, *J Appl Crystallogr*, 2020, **53**, 226–235.